THE ASTROPHYSICAL JOURNAL, 402:425–431, 1993 January 10

IMPLICATIONS OF LYMAN-ALPHA EQUIVALENT WIDTHS IN ACTIVE GALACTIC NUCLEI

JOSEPH C. SHIELDS AND GARY J. FERLAND
Department of Astronomy, Ohio State University, 174 West 18th Avenue, Columbus, OH 43210
Received 1992 March 16; accepted 1992 July 16

ABSTRACT

Variable Seyfert 1 nuclei exhibit a nonlinear response of Lyman α luminosity to changes in the continuum level, leading to a negative correlation between Lyα equivalent width and luminosity. We report the results of photoionization calculations that examine the sensitivity of Lyα emission to parameters describing the broad-line clouds and incident radiation field. The luminosity dependence of the equivalent width of Lyα can be understood in terms of increased destruction of the line at higher ionization parameter (U; ratio of ionizing photon to hydrogen density). The observed slope of equivalent width versus continuum flux for NGC 5548 and Fairall 9 is consistent with an ionizing continuum shape that is independent of luminosity. Measurements of the slope of Lyα equivalent width versus continuum brightness limit the permitted combinations of U and cloud density characterizing the Lyα-emitting zone.

We consider the case of the well-studied Seyfert 1 galaxy NGC 5548 and find good consistency with the observed properties of the Lyα zone for a cloud density of $\sim 10^{11}$ cm^{-3} and U near 0.2. Estimation of the cloud covering factor depends on the extrapolation of the extreme ultraviolet (EUV) continuum. EUV cutoffs at 20 and 60 eV correspond to a range of covering factors between 0.8 and 0.5, which is larger than typically assumed in the past for luminous Seyferts. Equivalent width observations of Fairall 9 show that its continuum cannot be as soft as suggested by previous line ratio analyses and imply that its EUV continuum persists to 20 eV or more before cutting off. Finally, we outline a method by which variability measurements can be combined with our calculations to measure the distances to active galactic nuclei, and hence the Hubble constant.

Subject headings: galaxies: active — galaxies: nuclei — galaxies: Seyfert — quasars: general — ultraviolet: galaxies

1. INTRODUCTION

Observational monitoring of variable Seyfert nuclei has convincingly demonstrated that emission from the broad-line region (BLR) correlates with changes in continuum luminosity in a manner consistent with photoionization of circumnuclear clouds by a central source (e.g., Clavel et al. 1991; Peterson et al. 1991). Emission-line luminosity does not scale linearly with the continuum level, however (Wamsteker & Colina 1986; Edelson, Krolik, & Pike 1990; Kinney, Rivolo, & Koratkar 1990; Pogge & Peterson 1992). Edelson et al. (1990) noted that nonlinear correlations are consistent in general terms with expected variations in the relative importance of different coolants at different luminosity levels. The detailed response of individual lines has received little scrutiny, however.

In this paper we report results of photoionization calculations that bear on the understanding of equivalent widths of Lyα in variable Seyfert nuclei. We find that the equivalent width versus luminosity behavior of this line imposes important constraints on the ionizing radiation field and on the properties of the BLR clouds.

2. PHOTOIONIZATION CALCULATIONS

2.1. *Preliminary Considerations*

In the simplest scenario for radiation-bounded clouds (i.e., clouds containing an ionization front), we would expect a balance between the rate of photoionizations and the rate of recombinations leading to emission of Lyα, so that the Lyα luminosity is directly proportional to the incident flux of hydrogen-ionizing photons, ϕ(H), given by

$$\phi(\mathrm{H}) = \int_{13.6\ \mathrm{eV}}^{\infty} \frac{4\pi f_\nu}{h\nu}\, d\nu\ . \tag{1}$$

Here f_ν is the flux per unit frequency interval, ν is photon frequency, and h is Planck's constant. The emitted Lyα flux for a given flux level in the local (1200 Å) continuum consequently depends on the continuum shape at ionizing energies. If we assume that each ionizing photon produces one Lyα photon, the equivalent width of Lyα [EW(Lyα)] will then be given by

$$\mathrm{EW(Ly}\alpha) = \frac{\phi(\mathrm{H})h\nu(\mathrm{Ly}\alpha)}{f_\lambda(1216)} f_c\ , \tag{2}$$

where f_c is the gas covering factor of a central source and $f_\lambda(1216)$ is the continuum flux (per unit wavelength interval) at Lyα. Larger equivalent widths are produced by harder continua (since the ratio $\phi(\mathrm{H})/f_\lambda(1216)$ is a direct measure of the mean photon energy) or larger covering factors. The equivalent width of Lyα measured across a photoionized cloud thus serves as a diagnostic of the ionizing continuum shape, which forms the basis for Zanstra techniques for the estimation of stellar temperatures in H II regions (e.g., Osterbrock 1989). If the continuum extending from 1216 Å through ionizing energies retains its spectral shape while changing in amplitude, then both Lyα from an irradiated cloud and the adjacent continuum are directly proportional to the incident flux of ionizing photons, implying that EW(Lyα) is independent of changes in continuum luminosity.

Measured EW(Lyα) for an active galactic nucleus (AGN)

could deviate from a constant value due to several complications to this simple picture. Light travel-time delays will introduce a phase shift between continuum fluctuations and the response of circumnuclear clouds; a detailed knowledge of the spatial distribution of clouds could in principle be used to remove this effect. The shape of the ultraviolet through soft X-ray continuum, which is poorly determined in AGNs, could also vary strongly as a function of luminosity. Such changes would cause variability in the Lyα line that is not commensurate with that of the local continuum. Measured line emission from such an idealized cloud could also be contaminated in real observations by nonvariable components within the observing aperture, such as would arise from an optically thin, fully ionized plasma, or an ensemble of clouds at large distance from the central source that shows no net response to changes in continuum luminosity. This effect would dilute variability in Lyα luminosity, so that Lyα would appear less variable than the continuum. Finally, Lyα may in reality be a nonlinear reprocesser of continuum radiation incident on the BLR clouds. Such a response might occur if the conditions leading to Lyα emission are decidedly nonnebular.

In order to examine the quantitative dependence of EW(Lyα) on parameters describing the emission-line clouds and radiation field, we carried out a series of calculations for conditions appropriate to the BLR and compare them here with observations of variable Seyfert nuclei.

2.2. *Computational Details*

Predicted emission-line spectra for a uniform, irradiated slab of gas were calculated using the code CLOUDY, version 80.05. The code treats atoms of hydrogen, the helium singlets, and the He^+ ion as 10-level atoms. In each case, levels 1–6 match the energy states of the true atoms, and three supplemental levels are chosen to mimic the average properties of high-n states. For conditions of interest here these levels are close to local thermodynamic equilibrium (LTE). The model atoms and ions go to the nebular limit under low-density conditions, and to LTE at high photon or particle densities. Further details are presented in Ferland (1991) and Ferland & Rees (1988).

Line transport with background opacities is treated using escape probabilities as in Hummer (1968; Lyβ and higher Lyman lines, and subordinate lines) and Hummer & Kunasz (1980; Lyα). In this formalism, atoms are depopulated from level $2p$ at a rate specified by $n_{2p} A_{2p,\,1s}(\epsilon + \delta)$, where ϵ is the escape probability and δ is the destruction probability. The former is (to zeroth order) inversely proportional to the line optical depth, while the latter is proportional to a parameter

$$X_c \equiv \frac{\kappa_c}{\kappa_c + \kappa_l}, \tag{3}$$

where κ_c and κ_l are the continuous and line opacities (with dimensions of cm^{-1}).

Stimulated emission and photoionization by the attenuated incident continuum are considered for all levels, and collisions and radiative transitions between all levels are included (Ferland & Rees 1988). Line emission is partially "destroyed" at a rate given by $n_u A_{ul} \delta$, and this process contributes a flux of on-the-spot (OTS) photons given by $\phi_{\rm OTS} = n_u A_{ul} \delta / \kappa_c$. All computed hydrogen and helium lines are included in this OTS field, and they contribute to ionization and heating of the gas, mainly through photoionization of excited states or free-free absorption.

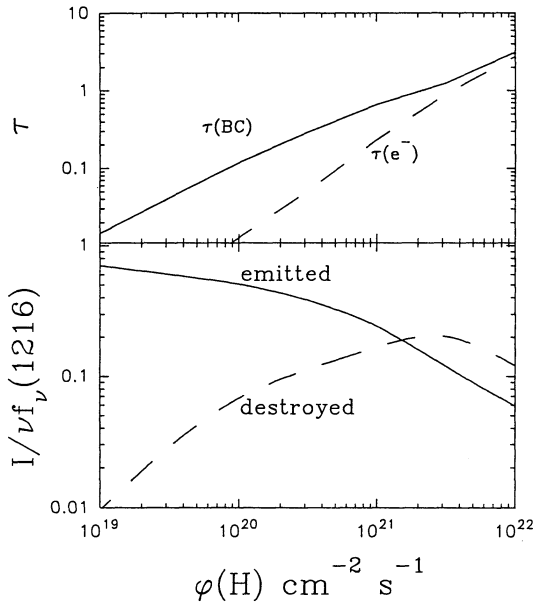

FIG. 1.—Calculation results for a cloud with $n_{\rm H} = 10^{11}$ cm^{-3} irradiated by an average AGN continuum with incident hydrogen-ionizing photon flux ϕ(H). The top panel shows the total optical depth in the Balmer continuum, as well as the optical depth due to electron scattering, as functions of ϕ(H). The ratio of Lyα luminosity to incident continuum luminosity at 1216 Å is shown vs. ϕ(H) in the bottom panel, for both emitted and destroyed components of the line.

Bound-free absorption of line emission becomes more important as ϕ(H) increases. As an illustration, Figure 1 shows the results of a series of calculations in which the hydrogen density was held constant at $n_{\rm H} = 10^{11}$ cm^{-3}, the calculations were stopped when the hydrogen ionization fraction reached 0.9, and the flux of ionizing photons was varied more than an order of magnitude to either side of the value inferred by Ferland et al. (1992) as representative of the C IV λ1549 region in NGC 5548. Solar abundances (Grevesse & Anders 1989) and the average AGN continuum shape from Mathews & Ferland (1987), with an added infrared cutoff longward of 10 μm, were assumed. At a given spot in the H^+ region the population of $2p$ is roughly set by the balance between recombination (with rate coefficient $\alpha_{\rm B}$) and radiative escape (proportional to $A_{21}\epsilon$). The escape probability for a radiation-bounded nebula is mainly proportional to the continuum shape and is of order 10^{-6} (Ferland & Netzer 1979).

Following Ferland & Netzer (1979), the density of $2p$ is then

$$n_2 = \frac{n_e n_+ \alpha_{\rm B}}{A_{21}\epsilon}, \tag{4}$$

and the optical depth in the Balmer continuum is proportional to this population integrated over the H^+ region, i.e.,

$$\tau({\rm BC}) \sim \sigma_{\rm BC} n_2 R_{\rm S}, \tag{5}$$

where $\sigma_{\rm BC}$ is the photoionization cross section at the Balmer edge. $R_{\rm S}$ is the Strömgren thickness of the H^+ region, given by

$$\phi({\rm H}) = R_{\rm S} \alpha_{\rm B} n_e n_+, \tag{6}$$

so that

$$\tau({\rm BC}) \propto \frac{\phi({\rm H})}{A_{21}\epsilon}. \tag{7}$$

The optical depth in the Balmer continuum determined from the point by point integrations of the full set of radiative and thermal balance equations is plotted in the upper panel of Figure 1, demonstrating that τ(BC) does increase in the expected manner and that the cloud is quite optically thick in the Balmer continuum for large values of ϕ(H). The optical depth to electron scattering, which is also proportional to ϕ(H), is also shown.

The lower panel of Figure 1 shows a quantity that is proportional to the equivalent width of Lyα. The number of created Lyα photons is, in the nebular limit, simply proportional to the intensity of the incident continuum for a radiation-bounded cloud, and the ratio (marked "emitted") would be constant if the continuum shape does not change. The line-to-continuum ratio drops as ϕ(H) increases because Lyα photons are increasingly lost to bound-free absorption from the $n = 2$ state. The "destroyed" intensity of the line ($n_2 A_{21} \delta$) is also shown in the figure.

As ϕ(H) increases, the opacity in the Balmer continuum (largely due to photoabsorption by hydrogen in the $n = 2$ level) also increases. The total optical depth in Lyα increases as well, but the optical depth characterizing most of the region of Lyα formation changes little (this is set by the constraint that we stop at the $H^+ - H^0$ ionization front). Thus the opacity ratio X_C and the destruction probability δ (which is proportional to X_C) increase, resulting in a decrease in EW(Lyα) as the clouds become less efficient reprocessors. Substitution of the escape probability with background opacity as formulated in Rees, Netzer, & Ferland (1989) results in predicted Lyα fluxes that are in good agreement with the treatment employed here, for selected test cases.

At the very largest values of ϕ(H) the cloud becomes optically thick to electron scattering. The plasma becomes a less efficient reprocessor of the incident continuum as the scattering optical depth increases and a larger fraction is reflected.

2.3. *Specific Applications*

In order to examine in detail the response of Lyα and other lines to properties of the ionizing continuum and BLR clouds, we computed the line intensities emitted under a variety of conditions, including irradiation by continua with shapes different from that assumed above. The incident continuum was described by an optical/UV power law with $\alpha = -0.5$ ($f_\nu \propto \nu^\alpha$), exponentially cut off above a variable extreme ultraviolet (EUV) energy (E_C; $10 \leq E_C \leq 60$ eV), and with a break to a power law with $\alpha = +2.5$ below 0.1 eV. The X-ray continuum was represented by a power law with $\alpha = -0.7$, steepening to $\alpha = -2$ above 50 keV. Mathematically, the continuum shape was thus described at optical through X-ray energies by $f_\nu = a\nu^{-0.5} \exp(-h\nu/E_C) + b\nu^{-0.7}$, where a and b are constants. The relative scaling of the optical and X-ray components was parameterized by α_{ox}, the spectral index connecting flux densities at 2500 Å and 2 keV (which differs here in sign from the usual convention), which we set equal to -1.4. Examples of the input spectra are shown in Figure 2. This description of the UV and ionizing continuum is consistent with typical active galactic nucleus properties (e.g., Elvis & Lawrence 1985; Mathews & Ferland 1987; Sun & Malkan 1989). The overall continuum level was adjusted such that the ionization parameter (U; ratio of ionizing photon and hydrogen densities) at the cloud face spanned a logarithmic range of -3 to $+0.5$ in increments of 0.5 dex. For each combination of parameters, the calculation was stopped at a column density corresponding to a fractional ionization of hydrogen of 0.9. Solar abundances were assumed. Resulting estimates of EW(Lyα) for $E_C = 20$ eV are shown in Figure 3 as a function of U, for hydrogen densities n_H spanning 10^9–10^{12} cm^{-3}, and full coverage ($f_c = 1$).

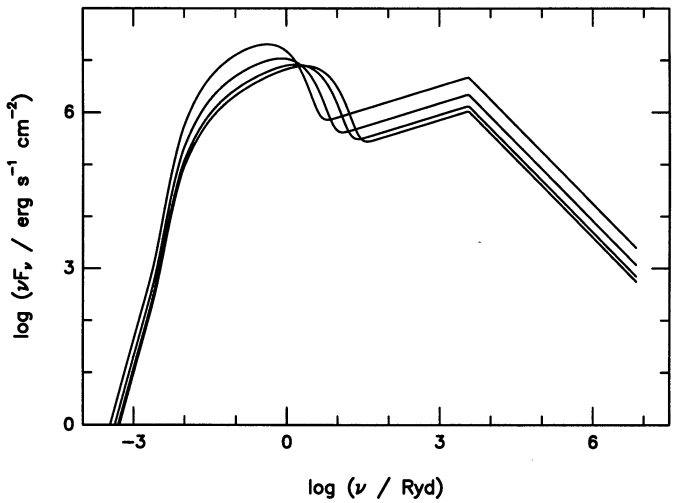

FIG. 2.—Incident model continua for log $U = -3$ and $E_C = 10$, 20, 40, and 60 eV.

3. RESULTS

Figure 3 illustrates that EW(Lyα) is inversely correlated with U and n_H, since ϕ(H) = $n_H U$ increases as either density or U is increased. This behavior can be explained by enhancements in the population of the $n = 2$ and other excited states of hydrogen as the timescales for photoionization and recombination shorten, leading to increased destruction of Lyα as the line photons are increasingly absorbed in photoionization. Increasing collisions and resulting thermalization of the line lead to additional decreases in EW(Lyα) at high density (cf. Rees et al. 1989). Comparison runs with E_C ranging from 10 to 60 eV indicate that the shape of the curves depicted in Figure 3 are insensitive to E_C, although they are translated vertically in this

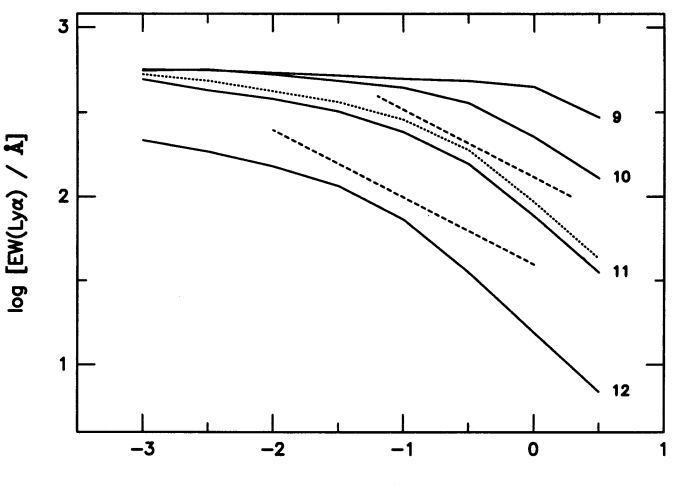

FIG. 3.—Equivalent width of Lyα as a function of U, for $E_C = 20$ eV. Separate curves correspond to the indicated values of log n_H. The dotted line represents the result for clouds with log $n_H = 11$ and 20 km s^{-1} microturbulence. Dashed lines are drawn with slope of -0.4 for comparison purposes.

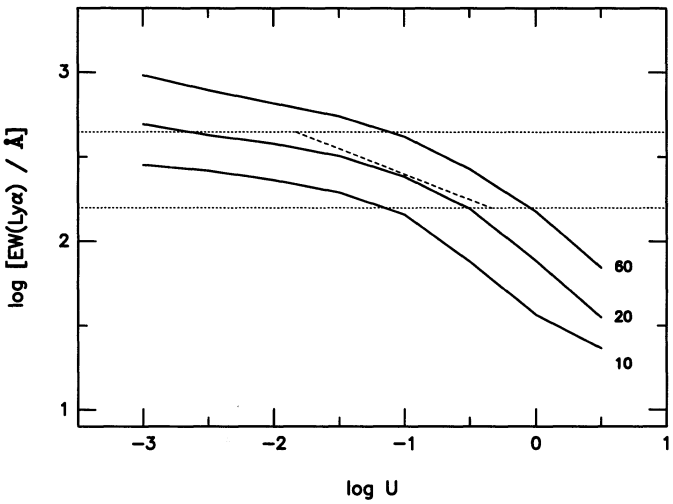

FIG. 4.—Equivalent width of Lyα as a function of U, for $n_H = 10^{11}$ cm^{-3}. Separate curves correspond to the indicated values of E_C in eV units. The dotted lines indicate the observed range of EW(Lyα) in Fairall 9, and the diagonal line indicates the observed slope for this object of −0.3.

plane such that continua with larger E_C have larger EW(Lyα), as expected (Fig. 4). The calculations for $E_C = 10$ and 60 eV differ by a factor of ~3.5 in the predicted EW(Lyα). Tests also indicate that these results are insensitive to choice of α_{ox}, except for very hard continua ($\alpha_{ox} \approx -1.0$) in which the X-ray power law is not a negligible contributor to ϕ(H).

Processes affecting the Lyα transport could modify the results plotted in Figure 3. An obvious candidate for such a process is velocity structure within the ionized cloud, which would facilitate increased Lyα leakage. To examine the consequences of line broadening, we repeated the calculation shown in Figure 3 for $n_H = 10^{11}$ cm^{-3}, with the irradiated plasma now characterized by a microturbulent velocity of 20 km s^{-1}, which is twice the Doppler width. The result is shown by the dotted line in Figure 3. As expected, EW(Lyα) increases at all U values, but by an amount $\lesssim$20%; the shape of the log EW(Lyα) versus log U curve is not significantly modified by this change. The leakage of Lyα could presumably be increased further if coherent transonic flows are important in the broad-line clouds, as could be the case, for example, if this material consists of stellar outflows.

The column density N_H of the ionized clouds will additionally affect EW(Lyα), since thinner clouds are less effective at reprocessing incident radiation. The criterion employed here of stopping the calculation when the fractional ionization of hydrogen is 0.9 results in a U-dependent column density; for example, log $U = -3$–$+0.5$ corresponds to $N_H \approx 10^{20}$–10^{24} cm^{-2}, assuming $E_C = 20$ eV and $n_H = 10^{11}$ cm^{-3}. Extending the calculation to a fractional ionization of 0.1 increases N_H in each case and also can change the resulting EW(Lyα). Figure 5 shows a comparison between the calculated EW(Lyα) when the calculation is stopped at a fractional ionization of 0.9 and 0.1. Extension of the calculation to higher N_H reduces the computed EW(Lyα) by $\lesssim$30%. A decrease in EW(Lyα) accompanying an increase in N_H may appear surprising, but results from increased destruction of Lyα photons as they scatter in the added regions of high optical depth.

The most physically relevant comparison to observations is likely to be for a model cloud of fixed N_H. Figure 5 also shows the results of a calculation extending through a cloud with hydrogen density of 10^{11} cm^{-3} and total $N_H = 10^{23}$ cm^{-2}. At low U, this depth exceeds that for a fractional ionization of 0.1, and EW(Lyα) is less than for either of the preceding test cases. The Balmer continuum optical depth initially increases with increasing U, but reaches a maximum and starts to decrease as the finite cloud becomes more ionized. The cloud becomes fully ionized at log $U \approx -0.5$, beyond which the Lyα luminosity changes little with increasing U, so that EW(Lyα) $\propto U^{-1}$, to good approximation.

The column density characterizing the broad-line clouds is unknown. Consequently, we use the results for calculations stopping at an ionization fraction of 0.9, with the understanding that these curves constitute an upper envelope to equivalent width predictions. The shape of the log EW(Lyα) versus log U curves is not strongly affected by the choice of N_H so long as the cloud remains optically thick. Associated changes in normalization are also small compared to those arising from different choices of E_C, as described above.

4. DISCUSSION

The discussion above suggests that the observed inverse relationship between EW(Lyα) and continuum brightness is a natural expectation for variable Seyfert nuclei. The curvature in the lines of constant n_H in Figure 3 implies that a quantitative comparison between observed and predicted power-law slopes for EW(Lyα) versus continuum luminosity could limit the permitted combinations of n_H and U if E_C is independent of luminosity. Alternatively, changes in E_C with luminosity might be implicated if a slope inconsistent with the calculated possibilities for fixed E_C is observed.

Pogge & Peterson (1992) have analyzed an extensive data set for NGC 5548, and quantified the power-law slope in the Lyα versus continuum luminosity plane for this source. Their slope should differ by a power of 1 from that in the log EW(Lyα) versus log U plane if continuum variations correspond to changes in U. This would be a plausible assumption if the cloud density and the separation between the central source and the Lyα clouds remain constant. After removal of time

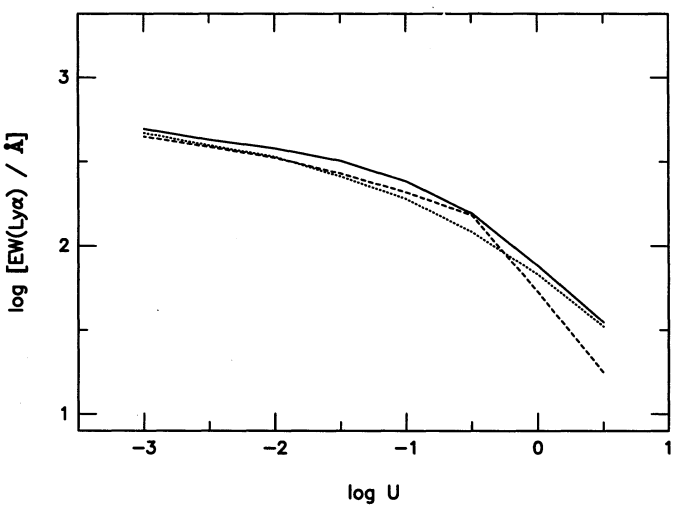

FIG. 5.—Equivalent width of Lyα as a function of U, for $n_H = 10^{11}$ cm^{-3} and $E_C = 20$ eV. The solid curve represents the result for calculations stopping at a fixed ionization fraction of 0.9. The result of extension of the calculation to an ionization fraction of 0.1 is shown by the dotted curve. The dashed curve represents predicted equivalent widths for a cloud with column density of 10^{23} cm^{-2}.

delays between the emission-line and continuum measurements, they find a slope of 0.5–0.6, corresponding to a measured slope of −0.4 to −0.5 in Figure 3.

This result is apparently not anomalous; we calculated the ordinary least-squares bisector (Isobe et al. 1990) for values of Lyα and 1335 Å continuum fluxes tabulated for Fairall 9 by Clavel, Wamsteker, & Glass (1989) and obtained a slope of 0.71 ± 0.05 (Fig. 6), corresponding to a slope of -0.29 ± 0.05 in Figure 3. The F9 data have the advantage of covering a range in luminosity of 1.6 dex, in contrast with ~0.6 dex for NGC 5548. However, the formal uncertainty in our result for F9 neglects the consequences of line-continuum time delays and measurement errors (see Pogge & Peterson 1992 for a discussion) and hence does not reflect the true uncertainty in this slope. The true uncertainty is probably large enough to provide agreement between the F9 and NGC 5548 slopes. The baseline over which U varies in F9 is sufficiently large that some curvature might be expected in its log EW(Lyα) versus log U relation, but the scatter in the measurements shown in Figure 6 apparently masks any such behavior.

Adopting a logarithmic slope of −0.4 for EW(Lyα) versus U as characteristic of active nuclei, or at least NGC 5548, we see from Figure 3 that this slope is indeed consistent with a continuum shape that is independent of luminosity. Assuming that E_C is thus constant, the measured slope can be used in combination with other constraints to limit the possible choices of U and density n_H that typify the Lyα zone. From inspection of Figure 3, the observed slope is matched for (log U, log n_H) of approximately (−1.25, 12), (−0.75, 11), and (−0.25, 10). The values of U at these points presumably correspond to a median brightness level for the varying source and are uncertain by approximately ±0.5 dex on account of uncertainty in the empirical slope. This identification of permitted U and n_H combinations, or equivalently, the incident ionizing photon flux, is virtually independent of properties of the radiation field such as α_{ox} and the value at which E_C is fixed, as well as the covering factor.

The density is additionally constrained by independent information concerning emission-line intensity ratios. The intensity ratio C III] λ1909/C IV λ1549 has been used in the past to argue for $n_H \lesssim 10^{10.5}$ (e.g., Davidson & Netzer 1979), but the realization that C III] is generated primarily outside of the Lyα–C IV zone (Clavel et al. 1991) has removed this stricture. Avoidance of C III] overproduction in the Lyα–C IV zone probably necessitates a density higher than this limit, in fact. Ferland et al. (1992) have employed this reasoning along with the requirement of avoiding overproduction of lines characteristic of very high densities to argue for a current best estimate of $n_H \approx 10^{11}$ cm^{-3}. Adoption of this density then implies in the present context that log $U \approx -0.75$.

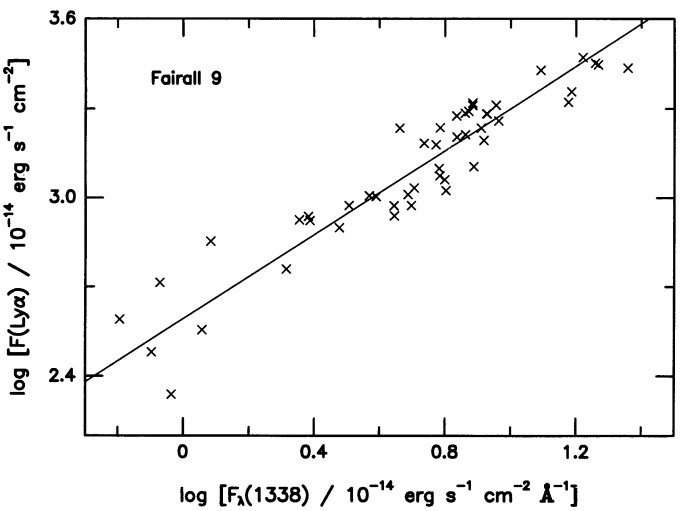

FIG. 6.—Flux of Lyα vs. continuum flux at 1338 Å for Fairall 9. The diagonal line represents the ordinary least-squares bisector, which has a slope of 0.71.

An additional consistency check on this combination of parameters is available for NGC 5548, in which the ionizing flux incident on the Lyα clouds can be directly estimated from time delays between continuum and line variations, in conjunction with an extrapolation of the ionizing continuum from the satellite UV region. By this means, Ferland et al. (1992) obtained a flux of ionizing photons corresponding to $\log(U \times n_H) \approx 10$ for a Hubble constant of $H_0 = 75$ km s^{-1} Mpc^{-1}, implying log $U \approx -1$ for $n_H = 10^{11}$ cm^{-3}. The disagreement of 0.25 dex between this estimate of U and that derived from the slope comparison is easily accounted for by uncertainties in the empirical log[EW(Lyα)]–log U slope and in the distance to NGC 5548 (which affects the direct flux estimate of U). In particular, the two determinations of U can be completely reconciled if we adopt $H_0 = 56$ km s^{-1} Mpc^{-1}, so that the direct flux estimate yields log $U \approx -0.75$. Further refinement of the measurements and modeling should provide a powerful method of directly measuring H_0. Application of this technique will require improved knowledge of the distribution of n_H and N_H as a function of radius. We note additionally that there is some uncertainty in a best value of line-continuum time delay used to directly estimate the flux incident on the Lyα clouds, since individual flaring events in NGC 5548 are characterized by time delays that may differ by as much as a factor of ~5 (Netzer & Maoz 1990).

If we thus adopt log $n_H = 11$ and log $U = -0.75$ as a consistent set of parameters for NGC 5548, we can determine the covering factor f_c of the Lyα–C IV clouds directly from a diagram such as Figure 3, since this number corresponds to the ratio of predicted (i.e., $f_c = 1$) and observed equivalent widths. Knowledge of f_c is important for the understanding of BLR structure and may have important implications related to the fact that some BLRs are hidden along selected lines of sight (e.g., Antonucci & Miller 1985). For NGC 5548, the median EW(Lyα) is ~160 Å (Pogge & Peterson 1992), while the predicted estimate for an incident continuum with $E_C = 20$ eV is ~200 Å, implying $f_c \approx 0.8$. As noted earlier, the predicted EW(Lyα) is an increasing function of E_C at a given U, such that f_c would decrease to ~0.5 for a fixed E_C of 60 eV. Covering factors of 0.5–0.8 are large compared to values previously assumed for luminous AGNs (e.g., Netzer 1990, and references therein).

The predicted EW(Lyα) and hence f_c obviously also depend more generally on the accuracy of our representation of the UV through EUV continuum, that is, the relative strength of the continuum at Lyα and the incident Lyman continuum. However, since U is almost invariably dominated by photons only slightly more energetic than the Lyman limit, which in turn is separated from Lyα by only 304 Å, large departures from our model continuum through this region are likely to be rare. The determination of f_c from this analysis thus requires primarily an additional constraint on E_C, which, of course, is of interest more generally for the understanding of AGNs. Mea-

surements of emission-line intensity ratios and the C IV λ1549/Lyα ratio in particular provide some prospects for constraining E_C (Shields & Ferland 1992). For $E_C = 20$ eV, emission-line intensities of other lines relative to C IV or Lyα appear to be generally consistent with observed ratios. Calculations with $\alpha_{ox} = -1.4$, $n_H = 10^{11}$ cm^{-3}, and log $U = -0.75$ yield line intensities for Lyα:He II λ1640:C IV λ1549:C III] λ1909:Mg II λ2798 of 1:0.053:0.64:0.069:0.019. For NGC 5548, a representative C IV/Lyα intensity ratio is ~0.9 (Pogge & Peterson 1992), which is high compared to most Seyfert galaxies; this value may implicate a somewhat higher E_C or U. For Fairall 9, a representative C IV/Lyα ratio is ~0.4. Obtaining detailed consistency with the emission-line spectra and hence determination of E_C for individual sources will require multizonal representations of the BLR that are beyond the scope of the present study.

Figure 3 can also be used, in principle, to exclude some combinations of parameters that would require an unphysical $f_c > 1$ to match an observed equivalent width. For example, an active nucleus with EW(Lyα) $\gtrsim$ 150 Å and characterized by a power law with slope of −0.4 in Figure 3 cannot be reproduced by a continuum with $E_C = 20$ eV and $n_H = 10^{12}$ cm^{-3}. More n_H–U combinations within the range of interest are excludable for lower E_C. For Fairall 9, Binette et al. (1989) and Clavel & Santos-Lleó (1990) have argued that the luminosity-dependent behavior of the C IV/Lyα intensity ratio requires a very soft $E_C < 13.6$ eV. If we estimate EW(Lyα) from Figure 6 for this object assuming that the continuum flux at 1338 Å is approximately equal to that at 1216 Å, EW(Lyα) ranged from approximately 160 Å to 450 Å as the nuclear continuum faded by a factor of ~30. If E_C remained fixed in this object at 10 eV, we can compare these measurements with the corresponding predictions of EW(Lyα) versus U (Fig. 7). Figure 7 indicates that the observed logarithmic slope in this plane can be matched with $n_H = 10^{11}$ cm^{-3} for median $U \approx 0.05$, but EW(Lyα) is underpredicted even if $f_c = 1$; i.e., the continuum is too soft to produce the required number of ionizing photons. Some improvement occurs if n_H is reduced to 10^{10} cm^{-3}, but

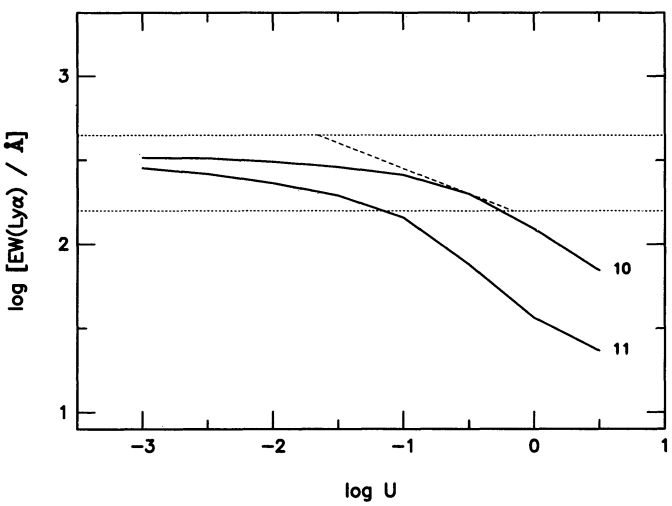

FIG. 7.—Equivalent width of Lyα as a function of U, for $E_C = 10$ eV. Separate curves correspond to the indicated values of log n_H. The dotted lines indicate the observed range of EW(Lyα) in Fairall 9, and the diagonal line indicates the observed slope in this plane of −0.3.

the agreement is still poor. This may constitute evidence for a harder EUV turnover, and, in fact, the predictions and observations are in considerably better agreement for $E_C = 20$ eV and f_c near 100%, or a higher E_C with lower covering factor (Fig. 4). A complication to this comparison is introduced by the fact that the observed α_{ox} was not constant for F9, but varied from approximately −1.4 in the high state to approximately −1.2 in the faint state (Clavel et al. 1989). Tests show that variation of α_{ox} over this range produces little change in computed EW(Lyα), however.

Previous estimates of f_c based on EW(Lyα) (e.g., Davidson & Netzer 1979) may be too low since they assumed lower values of n_H and U than are suggested by recent variability studies, and continua that may be harder than implied by α_{ox} measurements. Constraints on f_c have been derived from models of Balmer continuum emission (Wills, Netzer, & Wills 1985) and the incidence of Lyman-limit absorption (Davidson & Netzer 1979 and references therein), yielding $f_c \lesssim 0.5$ with significant uncertainties. X-ray studies have demonstrated that absorbing columns tend to be larger for objects with low hard X-ray luminosity (e.g., Lawrence & Elvis 1982). The column density within BLR clouds is likely to be large enough to introduce significant soft X-ray absorption; for example, log N_H corresponding to an ionization fraction falling to 0.9 for log $U = -0.5$, $\alpha_{ox} = -1.4$, and $E_C = 20$ eV, is 22.7, 23.1, 23.5, and 23.8 for log $n_H = 9$, 10, 11, and 12. The negative correlation between absorbing column and X-ray power might then reflect an inverse relation between f_c of the BLR and luminosity. Such a relationship may also be indicated by the Baldwin effect (Baldwin 1977), a negative correlation between broad-line equivalent width seen in Lyα (Kinney et al. 1990; Netzer 1990) and other emission lines, although alternative interpretations of this trend have been suggested (e.g., Netzer, Laor, & Gondhalekar 1992). As noted previously, covering factors of ~0.5 or perhaps higher for NGC 5548 and Fairall 9 are somewhat large compared to past estimates for luminous Seyfert nuclei; however, such f_c values are not clearly inconsistent with other data. In particular, both galaxies have 2–10 keV luminosities of ~10^{44} ergs s^{-1} (NGC 5548: Clavel et al. 1992; F9: Morini et al. 1986), which places them in the transition region from high to low f_c for AGNs (Lawrence & Elvis 1982).

5. CONCLUSIONS

The present photoionization calculations illustrate that the equivalent width of Lyα and its quantitative scaling with continuum luminosity in variable Seyfert nuclei constitute a significant diagnostic of physical conditions within the BLR. Measurements of NGC 5548 appear consistent with predictions that assume no variation in continuum shape as the luminosity of this source varies. The equivalent width behavior of this object is in agreement with independent suggestions that the emission-line clouds have a density of ~10^{11} cm^{-3} and nominal ionization parameter of ~0.2. For a given EW(Lyα), the cloud covering factor and cutoff energy of the big blue bump are inversely related; for a cutoff energy of 20 eV, the properties of NGC 5548 are reproduced with a covering factor of ~0.8. For Fairall 9, the observed equivalent width behavior may implicate a cutoff in the big blue bump at 20 eV or higher, which is inconsistent with suggestions of a very soft cutoff in order to explain the observed line ratio behavior. The present results provide additional motivation for the intensive spectro-

scopic study of variable AGNs, and for the quantitative measurement of the luminosity dependence of Lyα in particular, in order to characterize the physical parameters of the broad-line plasma. This information, combined with direct measurements of the luminosity of the underlying continuum, can be used to place constraints on the distances to AGNs, and hence H_0.

We thank B. Peterson and R. Pogge for useful discussions, and the referee, H. Netzer, for comments that resulted in improvements in the paper. E. Feigelson kindly provided software employed for regression in this study. This work was supported financially by NSF grant AST 90-19692 and NASA grant NAGS-1366.

REFERENCES

Antonucci, R. R. J., & Miller, J. S. 1985, ApJ, 297, 621
Baldwin, J. A. 1977, ApJ, 214, 679
Binette, L., Prieto, A., Szuszkiewicz, E., & Zheng, W. 1989, ApJ, 343, 135
Clavel, J., et al. 1991, ApJ, 366, 64
———. 1992, ApJ, 393, 113
Clavel, J., & Santos-Lleó, M. 1990, A&A, 230, 3
Clavel, J., Wamsteker, W., & Glass, I. S. 1989, ApJ, 337, 236
Davidson, K., & Netzer, H. 1979, Rev. Mod. Phys., 51, 715
Edelson, R. A., Krolik, J. H., & Pike, G. F. 1990, ApJ, 359, 86
Elvis, M., & Lawrence, A. 1985, in Astrophysics of Active Galaxies and Quasi-Stellar Objects, ed. J. S. Miller (Mill Valley: University Science), 289
Ferland, G. J. 1991, OSU Int. Rep. 91-01
Ferland, G. J., & Netzer, H. 1979, ApJ, 229, 274
Ferland, G. J., Peterson, B. M., Horne, K., Welsh, W. F., & Nahar, S. N. 1992, ApJ, 387, 95
Ferland, G. J., & Rees, M. J. 1988, ApJ, 332, 141
Grevesse, N., & Anders, E. 1989, in Cosmic Abundances of Matter (AIP Conf. Proc. 183), ed. C. J. Waddington (New York: AIP), 1
Hummer, D. G. 1968, MNRAS, 138, 73
Hummer, D. G., & Kunasz, P. B. 1980, ApJ, 236, 609
Isobe, T., Feigelson, E. D., Akritas, M. G., & Babu, G. J. 1990, ApJ, 364, 104
Kinney, A. L., Rivolo, A. R., & Koratkar, A. P. 1990, ApJ, 357, 338
Lawrence, A., & Elvis, M. 1982, ApJ, 256, 410
Mathews, W. G., & Ferland, G. J. 1987, ApJ, 323, 456
Morini, M., et al. 1986, ApJ, 307, 486
Netzer, H. 1990, in Active Galactic Nuclei, ed. T. J.-L. Courvoisier & M. Mayor (Berlin: Springer), 57
Netzer, H., Laor, A., & Gondhalekar, P. M. 1992, MNRAS, 254, 15
Netzer, H., & Maoz, D. 1990, ApJ, 365, L5
Osterbrock, D. E. 1989, Astrophysics of Gaseous Nebulae and Active Galactic Nuclei (Mill Valley: University Science)
Peterson, B. M., et al. 1991, ApJ, 368, 119
Pogge, R. W., & Peterson, B. M. 1992, AJ, 103, 1084
Rees, M. J., Netzer, H., & Ferland, G. J. 1989, ApJ, 347, 640
Shields, J. C., & Ferland, G. J. 1992, in preparation
Sun, W.-H., & Malkan, M. A. 1989, ApJ, 346, 68
Wamsteker, W., & Colina, L. 1986, ApJ, 311, 617
Wills, B. J., Netzer, H., & Wills, D. 1985, ApJ, 288, 94